Relative Strength of H-Bonding Groups on Biodegradable Polymer-Based Blends in Solution

V. Soria,[1] C. M. Gomez,[1] M. Falo,[1] C. Abad,[2] A. Campos[1]

[1]ICMUV-Departament de Química Física; Universitat de València, E-46100 Burjassot, València, Spain
[2]Departament de Bioquímica i Biología Molecular, Universitat de València; E-46100 Burjassot, València, Spaín

ABSTRACT: The intermolecular hydrogen bonding interactions between poly(3-hydroxybutyrate) and poly(styrene-*co*-vinyl phenol) copolymers with mutual solvent epichlorohydrin were thoroughly investigated by steady-state fluorescence and viscosity techniques. Fluorescence spectroscopy along with viscosity technique was used to asses the intermolecular hydrogen bonding between poly-(3-hydroxybutyrate) and its blends with five copolymer samples of styrene–vinyl phenol, containing different proportions of vinyl phenol but similar average molecular weight and polydispersity index. In the case of very low OH contents (2–4 mol %), as expected, both components of poly(3-hydroxybutyrate) and poly(styrene-*co*-4-vinylphenol) chains are well separated and remain so independently of the mixed polymer ratio and overall polymer concentration as well. Conversely, when the OH content reaches 5.8 mol % or more, a significant decrease of the intrinsic fluorescence intensity emitted by the copolymer is detected upon addition of aliquots of poly(3-hydroxybutyrate). In these cases, an average value for the interassociation equilibrium constant, $K_A = 8.7$, was obtained using a binding model formalism. A good agreement of these results with those obtained from complementary viscosity measurements, through the interaction parameter, Δb, was found. © 2006 Wiley Periodicals, Inc. J Appl Polym Sci 100: 900–910, 2006

Key words: poly(3-hydroxybutyrate); poly(styrene-co-vinyl-phenol); association constant

INTRODUCTION

It has been our interest to study ternary polymer solutions (TPS) dealing with a polymer in mixed solvents as well as two polymers in a common solvent. Recently, we are concerned on TPS with specific interactions taking place by hydrogen bonding, as an extension the of preceding thermodynamic studies on binary and ternary interactions.[1–3] It is well known that H-bonding plays a crucial role in determining the physical and thermodynamic properties of polar fluids.[4,5] For example, in the domain of polymer blends, an immiscible polymer pair can be transformed into a miscible one by enhancement of the thermodynamic compatibility, which can be realized as the intermacromolecular H-bonding complexation is intensified.[6,7] A powerful tool to detect specific interactions in polymer blends is Fourier transform infrared (FTIR) spectroscopy. Observed changes in hydroxyl, carbonyl, and ether vibrations provide direct evidence of H-bonding specific interactions between blend components.[7,8] The magnitude of the shift in wave number,

arising due to blend formation, yields a measure of the average strength of the intermacromolecular interactions. In addition, other techniques such as nonradiative energy-transfer (NRET) fluorospectroscopy, laser light scattering (LLS), thermal analysis (DSC), NMR-NOE, electronic microscopy, inverse gas chromatography, and viscometry have been used to study polymer–polymer miscibility or compatibility both in solid state and in solution.[9–15]

In this context, we have chosen as model compounds a set of five in-house-made poly(styrene vinyl phenol) copolymers, a commercial sample of poly(3-hydroxybutyrate) (PHB), and a common solvent such as epichlorohydrin. The PHB used here is an isotactic naturally occurring thermoplastic polyester belonging to the family of biodegradable poly(hydroxyalkanoate)s.[16] Binary blends of PHB with other synthetic polymers has attracted much interest as one approach to improve the inherent brittleness as well as to reduce high production cost of these polyesters. In this way, much work on blending it with other nonbiodegradable polymers such as poly(vinyl acetate),[17] poly-(methyl methacrylate),[18] poly(epichlorohydrin)[19,20] as well as biodegradable polymers such as poly(ethylene oxide),[21] poly(vinyl alcohol),[22] poly(ε-caprolactone),[23] and polysaccharides[24] has been reported. In addition, mixtures with synthetic (amorphous) PHB as well as bacterial (tactic) PHB were also considered. An excellent review on the miscibility, properties, and biode-

gradability of microbial polyester containing blends, including PHB polymers and copolymers, has been recently reported.[25]

On the other hand, polystyrene (PS) is an important commodity polymer, which has been thoroughly studied in the literature in contrast with the poly(vinyl phenol) (PVPh), for which commercial uses are limited to the field of photoresistance.[26] Obviously, it is well known that PS is incompatible with the PHB, whereas the PVPh is compatible and miscible both in solid state and in solution, in a whole composition range.[27] This miscibility has been attributed to specific hydrogen-bonding interactions between the carbonyl groups of the PHB and the hydroxyl groups of the PVPh.[28,29] PS has almost the same chemical structure as PVPh but lacks the H-bond forming OH group in the para position of the aromatic cycle that gives PVPh its hydrogen-bonding ability. To mitigate PS–PHB incompatibility, we have slightly modified the PS chains, by insertion of small amounts of vinyl phenol groups in the PS backbone, via radical copolymerization. Therefore, copolymers of styrene and vinyl phenol (in small amounts) are expected to display physicochemical, rheological, and mechanical properties close to those of PS homopolymer.

The aim of this work is to study the composition effect of statistical styrene vinyl phenol copolymers (PSVPh) on the compatibility of PHB/PSVPh blends in dilute ECH solutions. Thus, the analysis of the effect of hydrogen bonding on the compatibility will be investigated using fluorescence intensity and viscosity measurements of these polymer mixtures in epichlorohydrin as common solvent. The changes in fluorescence intensity were used to obtain association isotherms as a function of polymer mixture composition as well as mol % groups of vinyl phenol in the PSVPh copolymer. To quantitatively interpret the association isotherms, a binding model[30–33] has been used, allowing us to obtain an intermolecular association constant representative of the extent H-bonding attractive interactions between both polymer samples. Dilute solution viscosity measurement of mixed polymer solutions has proved to be a useful technique to investigate polymer–polymer interactions,[14,15,34–38] so that solution viscometry has also been used to elucidate interpolymer complexation in solution.[39] Here, we have used the so-called polymer-solvent method[34,37,40] to evaluate PHB–PSVPh interactions in ECH as solvent, by means of the Δb parameter introduced by Krigbaum and Wall for polymer–polymer–solvent ternary systems (TPS).[41]

EXPERIMENTAL

Materials

Epichlorohydrin (1-chloro-2,3-epoxypropane) was obtained from Panreac Quimica S.A.(Barcelona, Spain);

styrene, 4-acetoxystyrene, hydrazine hydrate, and isotatic poly(3-hydroxybutyrate) were purchased from Aldrich Chemical; methanol was purchased from Baker BV (Deventer, Holland); $\alpha\alpha'$-azobis(isobutyronitrile) (AIBN) was purchased from Fluka Chemie AG (CH) and tetrahydrofuran (THF) from Scharlau Chemie S.A. (Barcelona, Spain). Monomers were purified by vacuum distillation before use. All other chemicals were used as-received.

Synthesis of poly(styrene-*co*-4-vinylphenol) copolymers

Poly(styrene-*co*-4-vinyl phenol) (PS-*co*-VPh) random copolymers with different mole % VPh were prepared by the free-radical polymerization of styrene and 4-acetoxystyrene using AIBN as the initiator, followed by the hydrolysis of the acetoxy groups, using hydrazine hydrate, according to the procedure of Khatri et al.[42] Hereinafter, PSVPh(n) denote a PS-*co*-VPh random copolymer with n mol % VPh. An example for the synthesis of PSVPh(7) copolymer is shown below. First, styrene (40 g), 4-acetoxystyrene, and AIBN (0.3 g) were transferred into a three-neck round-bottom flask filled with toluene (50%, w), under a mild flow of nitrogen. The flask equipped with a water-jacketed condenser was heated at 60°C for 12 h. The solution was then poured into a methanol–tetrahydrofuran mixture to precipitate the poly(styrene-*co*-acetoxystyrene) as the product. The polymer was dried in a vacuum oven for 1 day. Next, the hydrolysis of acetoxy groups to hydroxyl groups was carried out by dissolving 2.5 g of poly (styrene-*co*-acetoxystyrene) in dioxane (50 mL) in a round-bottom flask. Hydrazine hydrate (8 mL) was then added to this solution and stirred for 40 h at room temperature. The polymer was precipitated into methanol and dried in a vacuum oven for 24 h. Resulting conversions were about 10%.

Polymer characterization

Molecular weight and polydispersity index of the polymers were determined by size exclusion chromatography (SEC), using a Waters gel permeation chromatograph equipped with a refractive index detector. A solution of PHB in ECH was injected throughout a set of three TSK super AW columns (Toso Co.; Tokyo, Japan) and the five PSVPh copolymer samples were diluted in THF and eluted throughout a set of three TSK gel HXL columns (Toso). The eluents were always filtered and degassed through regenerate cellulose filters of 0.45-μm pore diameter (Micro Filtration System; Dublin, CA, USA). The mobile phase flow rate was adjusted to 0.5 mL/min and sample injection volume was 100 μL in all cases. PS with a narrow molecular weight distribution was used as calibration standard for all polymers. Data collection and han-

TABLE I
List of Polymers Used and Sample Characteristics

Sample	OH content (mol %)	M_n (10^3 g/mol)	M_w/M_n	$[\eta]$ (mL/g)	K_H
PHB	—	245	1.51	212.8	1.23×10^{-2}
STVPh2	2.0	33.7	1.78	31.5	-24.2×10^{-2}
STVPh3	3.2	34.3	1.78	—	—
STVPh4	4.0	35.0	1.77	33.2	$-23.4\ 10^{-2}$
STVPh6	5.8	36.7	1.77	34.4	$-6.92\ 10^{-2}$
STVPh7	7.2	36.7	1.77	35.5	$-6.06\ 10^{-2}$

dling were carried out using Millenium GPC Software from Waters (Milford, MA, USA).

The vinyl phenol content for each PSVPh sample was analyzed by ^{1}H NMR spectroscopy. ^{1}H NMR spectra were recorded at room temperature on a Varian Unity 300 spectrometer (300 MHz), using CDCl$_3$ as solvent and tetramethylsilane as an internal chemical shift reference. Table I lists the molecular weight characteristics for the homopolymer PHB and for five PSVPh copolymers, as well as the content (mol %) in vinyl phenol for each copolymer sample.

Fluorescence measurements

Fluorescence emission spectra of PSVPh polymer solutions were recorded at room temperature (~25°C), on a Aminco-Bowman Luminiscence Spectrometer, using a 1-cm quartz cell. The excitation wavelength was set at 260 nm, and the fluorescence emission spectra were monitored from 280 to 380 nm. The component polymer solutions were prepared with oxygen-free solvent. Titrations were performed by addition of small aliquots of the PHB solution to the PSVPh at a desired concentration in organic solvent, and the data shown are representative of several independent experiments. The concentration of PSVPh in the blend solution was kept at 5.0×10^{-4} g/mL and varying the PHB concentration, covering from 0 to 3.5 the molar ratio R_i (= [PHB]$_T$/[PSVPh]$_T$). Polymer solutions were placed in the quartz cell, stirred for 10 min, and purged with nitrogen for at least 1 min prior to each recording.

Viscosity measurements

An AVS 440 Ubbelohde-type viscometer from Schott Geräte (Hofheim, Germany) was used to determine the relative viscosities of the individual polymers and blends in epichlorohydrin as common solvent. In all experiments, a 15 mL sample at 1.0% (w/v) concentration was loaded into the viscometer, which was then placed into a thermostated bath at 25 ± 0.02°C. Measurements were initiated after approximately 5–10 min equilibrium time and were continued until several elution time readings agreed to within 0.5%. Viscosity of ternary polymer systems was carried out

using the polymer solvent method. A controlled weight of PHB was dissolved in a dilute solution of PSVPh–ECH at two constant concentrations of PSVPh, namely 1×10^{-3} and 0.5×10^{-3} g/mL, respectively. Flow times of each ternary system were determined by the serial dilution technique. Five dilutions were made for each polymer mixture composition and an extrapolation procedure was used to evaluate the corresponding intrinsic viscosity and the Huggins constant. Kinetic energy corrections were applied.

RESULTS AND DISCUSSION

We are interested in quantitatively estimating the extent of intermolecular hydrogen bonding between PHB and PSVPh(n) chains with the goal of finding a miscible blend by optimizing this parameter. Altering the composition of an amorphous copolymer, such as the PSVPh(n), systematically varies the extent of intermolecular hydrogen-bonding between the two components. The PHB has its carbonyl group interaction site localized in each monomer unit, while PSVPh(n) copolymer can change its hydroxyl interaction site content. This enables us to explore the functional group content dependence on complexation process.

Figure 1 shows the SEC elution profiles for PSVPh(4), PSVPh(6), and PSVPh(7) copolymers in TSK gel HXL columns. PSVPh(2) and PSVPh(3) samples are not shown here for simplicity, since their profiles are practically superposed to those depicted here. From the elution profiles the values of M_w and M_n as well as the polydispersity index were evaluated. These values are summarized in Table I for each polymer sample. The number following PSVPh represents the approximate integer value of the molar content of 4-vinylphenol in the copolymer. In the second column the copolymer composition in mol % of vinyl phenol, determined by ^{1}H NMR as detailed in the Experimental section, are compiled. Notice that to blend PHB with a commodity like polystyrene copolymer, a narrow range of VPh content in the PSVPh, namely from 2 to 7.2 mol %, was assayed. However, in some reports, involving hydrogen-bonding compatibilization of PSVPh-based blends, the copolymer composition exceeds hardly the above range. Obviously, the physical properties of these samples, at least for high vinyl
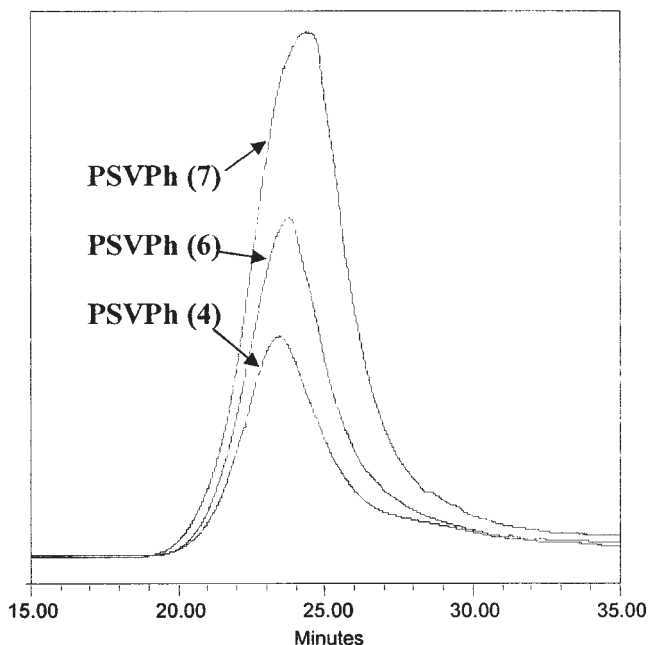
Figure 1 SEC traces of PS-*co*-VPh in THF at room temperature.

phenol content, cannot be considered as those commercial polystyrene, which are widely recognized as a commodity polymer. Lastly, columns three and four refer to the molecular weight and uniformity features. As can be seen, almost PSVPh have similar M_n, close to 35 kg/mol, and a high degree of uniformity, $U = (M_w/M_n) - 1$, close to 0.775 in all cases.

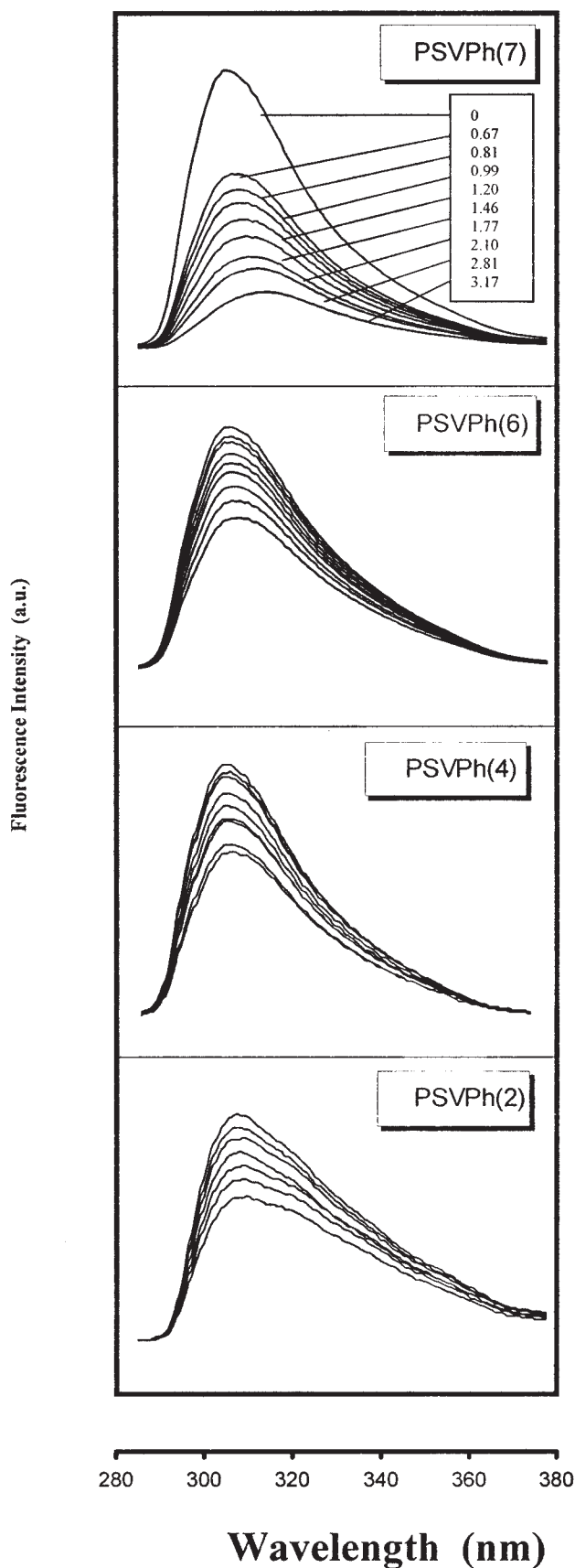### Fluorescence monitoring of polymer–polymer interaction

Figure 2 shows the fluorescence emission spectra of the different PSVPh copolymers upon addition of PHB in ECH as solvent. In general, the fluorescence spectra of the copolymers show a broad emission band in the region of 290–370 nm. High peak evolution for the fluorescent polymer, PSVPh, upon addition of aliquots of a nonfluorescent polymer as PHB, are clearly significant for both PSVPh(6) and PSVPh(7), whereas a weak interpolymer interaction is experimentally observed for the remaining PSVPh-PHB blends. The emission maximum for pure PSVPh(7) solution in ECH, denoted by $R_i = 0$ is centered at 302 nm wavelength. In addition, a bathochromic red-shifted effect appears as the R_i values increase, the maximum peak emission for PSVPh(7)–PHB blend being detected close to 313 nm for $R_i = 3.17$. A similar behavior, but less pronounced, can be assigned to PSVPh(6)–PHB solutions. The red-shift, which is indicative of fluorophore sequestration in a more polar environment, can be related to a stabilization of the excited state by polymer–polymer interaction via H-bonding.

Altering the composition of an amorphous copolymer, such as PSVPh(n), systematically varies the extent of intermolecular H-bonding between the two components. In our case n varies from 2.0 to 7.2 mol %. If the hydroxyl groups containing PSVPh are too dilute, insufficient interacting moieties exist, being the intermolecular bonds very limited, as can be seen at the bottom of Figure 2, where the fluorescence signal for PSVPh(2) is practically independent of the R_i values. Conversely, when the OH content increases, the H-bond specific interactions become evident and the fluorescence intensity of PSVPh decrease as PHB concentration increase, raising the top value for $n = 7$. This behavior may be understood in terms of two competitive effects as follows.[43,44] On the one hand, increasing the spacing of the phenol groups along the copolymer chain, i.e. decreasing the n value, we provide the necessary rotational freedom to allow the hydroxyl groups of PSVPh to find and properly orientated relative to the carboxyl group of the PHB sample. On the other hand, increasing the n values until $n = 7$ as it has been done here or, for instance, until $n = 50$ as it has been recently reported for the same polymer pair in solid state,[50] the rotational freedom can be seriously restricted. Thus, it seems to be plausible to accept that optimum number of H-bonds occurs when both rotational freedom and the PSVPh copolymer composition, n, are balanced.

From these spectra, the observed intensity value, I, can be assigned to the emission of both free $[PSVPh]_F$ and bound $[PSVPh]_B$ copolymers, that are present in solution at a total concentration: $[PSVPh]_T = [PSVPh]_F + [PSVPh]_B$. It can be easily deduced that[46]

$$I = \frac{[PSVPh]_B}{[PSVPh]_T} I_B + \frac{[PSVPh]_F}{[PSVPh]_T} I_0 \qquad (1)$$

I_B being the fluorescence intensity for PSVPh totally bound to PHB sample (not directly obtained from the spectrum) and I_0 the fluorescence intensity of PSVPh–ECH solutions in the absence of PHB. The I_0 values are compiled in Table II, which has been deduced from the fluorescence spectrum depicted in Figure 2 at 302 nm for $R_i = 0$. To follow the spectral changes quantitatively, the variation of the fluorescence intensity of PSVPh as a function of the ratio R_i is plotted in Figure 3, for the different polymer mixtures. As expected, the fluorescence intensity decay was observed for all the PSVPh samples. The extent of intensity decrease is, of course, a function of both R_i and n, which is closely related with the amount of –OH. . . O=C< local specific interactions. Notice that PHB polymer is only active as sample acceptor, altering the fluorescence quantum yield of the PSVPh itself when the linkage via H-bonding between the PHB and PSVPh take place. Additional fluorescence experiments (not shown), with the same PSVPh–ECH solutions in the

| 0 |
| 0.67 |
| 0.81 |
| 0.99 |
| 1.20 |
| 1.46 |
| 1.77 |
| 2.10 |
| 2.81 |
| 3.17 |

PSVPh(7)

PSVPh(6)

PSVPh(4)

PSVPh(2)

Fluorescence Intensity (a.u.)

280　300　320　340　360　380

Wavelength (nm)

presence of fully inert (macro) molecule, e.g., *n*-hexane, confirm what has been stated earlier, where any PSVPh sample depict the same fluorescence quantum yield independent of the R_i values. At very low OH content, the fluorescence intensity decay varies poorly with R_i for PSVPh(2) sample, which can be attributed to the scarce linkages between both polymers. In contrast, at high OH content, this variation is very pronounced (see PSVPh(7) sample) even at R_i values lower than 1. This behavior shows that the H-bonding links between the complementary functional groups of both polymer samples become highly favorable.

Equation (1) can be rewritten as follows:

$$I = \alpha I_B + (1 - \alpha)I_0 \qquad (2)$$

where α is the fraction of PSVPh bound to PHB and where $(I-\alpha)$ is the fraction of PSVPh free in solution. From eq. (2), α can be evaluated from the experimental data:

$$\alpha = \frac{I - I_0}{I_B - I_0} \qquad (3)$$

As explained above, I and I_0 are directly obtained from the fluorescence spectra (see Table II), while I_B has to be deduced from the so-called double reciprocal plot,[33]

$$\left(\frac{I - I_0}{I_0}\right)^{-1} = \frac{I_0}{I_B - I_0} + \frac{I_0 N}{(I_B - I_0)K_A^* r[\text{PSVPh}]_T}R_i^{-1} \quad (4)$$

K^*_A represents an apparent association constant between both polymers and r the polymerization degree of PHB. Because the treatment remains identical to those earlier given,[30–32,45] we will not reproduce in this contribution a deduction in depth of this equation. Figure 4 shows the plot of $I_0/(I-I_0)$ versus I/R_i for the PHB–PSVPh mixtures in ECH, where a good correlation is found in all cases allowing us to obtain a linear correlation fit. Because I_0 is known, from the intercept of this plot one can obtain the I_B values for each PSVPh copolymer. Now, it is a relatively straightforward task to calculate the α values from eq. (3) for each PHB–PSVPh–ECH system. In Table II these α values are compiled for different polymer concentration ratio, R_i, for each PSVPh copolymer. Inspection of these results reveals that at a fixed R_i polymer ratio, the α values monotonically increase as the OH groups in the PS-

Figure 2 Typical fluorescence spectra of PS-*co*-VPh samples in epichlorohydrin as a function of polymer/polymer molar ratio, R_i = [PHB]/[PSVPh] at 25°C. The excitation wavelength was set at 260 nm. The range of R_i values covered in all experiments are depicted at the top of this plot.

TABLE II
Experimental Values of the Peak Emission Intensity, I, in arbitrary units, and Molar Fraction of PSVPh (n) Bound to PHB, α, from Fluorescence Measurements at Different Polymer Molar Ratio, R_i

[PHB] (10^3 g/mL)	R_i (mol/mol)	PSVPh(7)		PSVPh(6)		PSVPh(4)		PSVPh(3)		PSVPh(2)	
		I	α	I	α	I	α	I	α	I	α
0.0	0.00	107.61	—	82.94	—	78.65	—	59.43	—	63.96	—
1.9	0.67	73.54	0.25	71.21	0.15	70.02	0.09	56.25	0.06	57.03	0.05
2.3	0.81	67.81	0.29	68.34	0.18	70.03	0.09	55.99	0.07	54.21	0.07
2.8	0.99	62.02	0.34	66.98	0.20	68.77	0.11	54.71	0.09	54.14	0.07
3.4	1.20	57.01	0.37	63.67	0.24	64.05	0.16	53.77	0.11	55.02	0.06
4.1	1.46	50.63	0.42	60.97	0.27	60.68	0.20	52.33	0.14	53.34	0.08
5.0	1.77	44.08	0.47	58.47	0.30	57.21	0.23	52.72	0.13	50.02	0.10
6.1	2.15	36.33	0.53	54.40	0.35	56.53	0.24	49.68	0.20	49.12	0.11
7.4	2.61	32.08	0.56	50.12	0.41	50.27	0.31	49.65	0.20	46.27	0.13
9.0	3.17	23.06	0.63	45.49	0.46	48.22	0.33	48.61	0.22	42.26	0.16

VPh increase, denoting that the fraction of PHB bound through H-bonding to the PSVPh also increases. Neither of the systems assayed here reaches saturation, which enables to assume that the higher OH content in the PSVPh copolymer the higher the association is, scaling α to 0.63.

The binding model

Because interpolymer complexation between complementary groups placed on two unlike polymer chains can often be considered as typical equilibrium in solution, we have used an earlier developed binding model.[45] Therefore, we will consider a solvent in the presence of two interacting polymers. In this framework, the following equilibrium can be assumed:

$$P + S_N \rightleftarrows PS_N \qquad (5)$$

Being P the proton donor or PSVPh chainlike unbounded, S_N the proton acceptor, corresponding to a PHB site and PS_N standing for the PSVPh–PHB complex. Here, a site is constituted by N polymer segments or carbonyl groups that take part in the cooperatively rearranging volume around a PHB coil and able to interact with a proton donor molecule. Therefore, given the specific nature of the complexation and the large size of the PHB chain relative to the PSVPh copolymer, it seem to be realistic to take into account the possibility of overlapping binding sites. Because we have assumed in the equilibrium given by eq. (5) that a PSVPh molecule interact with a PHB site, one molecule of PHB will interact with (r/N) PSVPh molecules. In other words, (r/N) represent the number of sites on the nanoscale level by macromolecule of PHB.

This approach has of course severe restrictions. First, this model does not account for self-associating species. Therefore, the self-association of hydrogen-bonded hydroxyl–hydroxyl such as dimers, trimers, and multimers, only dominant at higher vinyl phenol content and included in other association models,[7,8] are not contem-
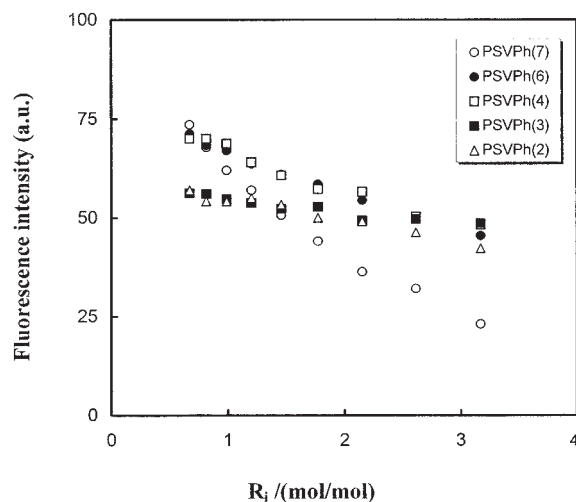
Figure 3 Fluorescence emission intensity as a function of polymer molar ratio, R_i, for different PSVPh samples.
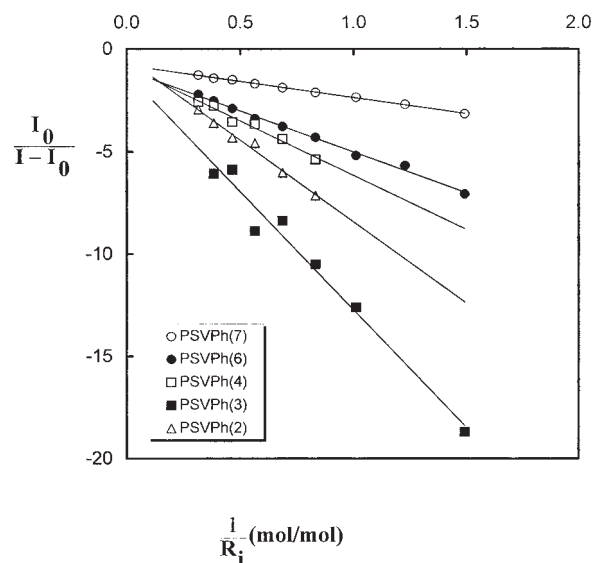
Figure 4 Plot of eq. (4), for different PSVPh samples.

plated in our scheme. The aforementioned assumption has been experimentally validated in mixtures of low molecular weight analogues, where at low alcohol concentrations (mol fraction, $x_{\text{alcohol}} < 0.0005$), alcohol is unable to self-associate.[46] Taking into account the effect of copolymer composition, the interassociation hydroxyl–carbonyl becomes dominant at lower vinyl phenol content in PSVPh because the small numbers of the hydroxyl groups in the copolymer tend to interact completely with carbonyl groups. Second, the acceptance of the Equation (5) also assumes that the association between unlike polymers is independent of the chain length, which is not strictly true for phenols and alcohols, where there are cooperative effects. Since these effects are expected to be highly nonuniversal, it is not easily quantified through standard theoretical approaches.[47–49] Therefore, the simplified binding model used here, does not capture the intramolecular screening effect, so that inclusion of the cooperativity in our formalism is beyond our scope.

We can now turn our attention upon eq. (5), where a characteristic association constant, K_A, of the above equilibrium can be expressed as

$$K_A = \frac{a_{PS_N}}{a_P \cdot a_{S_N}} = \frac{[\text{PSVPh}]_B}{[\text{PSVPh}]_F \cdot [S_N]} \qquad (6)$$

a_{PSN}, a_P, and a_{SN} are the corresponding activities. For simplicity and taking into account that the real polymer solutions used here fall always into the dilute polymer solutions regime ($c < [\eta]^{-1}$), we have approached the activities to molar concentrations. $[S_N]$ denotes the concentration of unoccupied sites at equilibrium, each one constituted by N carbonyl groups. In addition, $[S_N] = [S_T] - [PS_N]$ where $[S_T]$ refers to the total concentration of binding sites and $[PS_N]$ is the concentration of interpolymer complexes, which can be expressed as $[\text{PSVPh}]_B = \alpha[\text{PSVPh}]_T$. The $[S_T]$ can also be expressed as the ratio between the total number of carbonyl groups by volume, $r[\text{PHB}]_T$, and the number of carbonyl groups by site, N, being r the PHB polymerization degree. Taking into account the above relationships, the equilibrium constant, K_A, can be rewritten, as a function of experimental data obtained from spectroscopic fluorescence measurements, as follows[30,45]:

$$K_A = \frac{\alpha[\text{PSVPh}]_T}{[\text{PSVPh}]_F \left\{ \dfrac{r[\text{PHB}]_T}{N} - \alpha[\text{PSVPh}]_T \right\}} \qquad (7)$$

Recalling that $(\alpha/R_i) = \alpha[\text{PSVPh}]_T/[\text{PHB}]_T$, eq. (7) can be easily transformed into:

$$K_A = \frac{\alpha/R_i}{[\text{PSVPh}]_F \left\{ \dfrac{r}{N} - \dfrac{\alpha}{R_i} \right\}} \qquad (8)$$
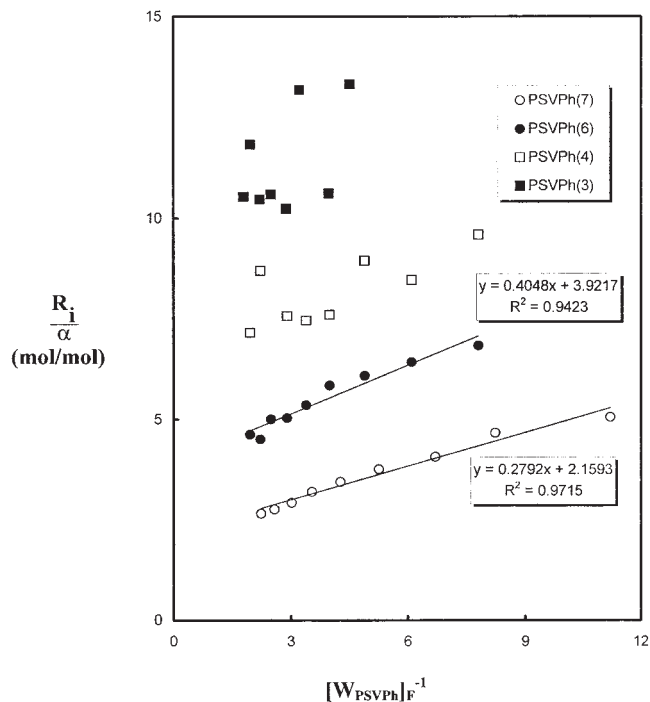

Figure 5 Plot of the eq. (11). Linear fit data are labeled on the corresponding system.

By rearranging, under the Langmuir isotherm mode, the following is obtained:

$$\frac{\alpha}{R_i} = \frac{\dfrac{r}{N} K_A[\text{PSVPh}]_F}{1 + K_A[\text{PSVPh}]_F} \qquad (9)$$

This equation can easily be linearized by inversion of both sides,

$$\frac{R_i}{\alpha} = \frac{N}{r} + \frac{N}{rK_A}[\text{PSVPh}]_F^{-1} \qquad (10)$$

Moreover, to estimate a dimensionless equilibrium constant, K_A, as it is specified by other models,[7,8] we have written the PSVPh composition as weight fraction, w_{PSVPh} in place of molar concentration

$$\frac{R_i}{\alpha} = \frac{N}{r} + \frac{N}{rK_A}(w_{\text{PSVPh}})_F^{-1} \qquad (11)$$

The plot of the R_i/α versus $[w_{\text{PSVPh}}]_F^{-1}$, according to eq. (11), shown in Figure 5 provides information on the effect of copolymer composition on the extent of intermolecular hydrogen-bonding, for five PSVPh samples blended with PHB in ECH as mutual solvent. In this figure, the data are well regressed linearly in the whole composition range for the ternary systems containing PSVPh(6) and PSVPh,(7) supporting the validity of eq (5). However, a gross scatter of points

without correlation is found for the remaining TPS, confirming in these cases the weakness of hydrogen bonding interactions or the absence of interpolymer linkages. Values of the intercept (N/r) and slope (N/rK_A), according to eq. (11), were calculated for TPS with linear correlation, being the values of the dimensionless equilibrium association constant, $K_A = 9.7$ for PSVPh(6) and $K_A = 7.7$ for PSVPh(7), at 25°C, respectively. In addition, the ratio (N/r) can also be estimated from the intercept, being 3.9 and 2.1 for the ternary systems containing the above PSVPh samples, respectively. At light of these (N/r) values, it can be stated that a single PSVPh(6) macromolecule could be interact simultaneously with four PHB coils and a PSVPh(7) macromolecule with two PHB coils.

The comparison of the K_A values obtained reveals that the higher the vinyl phenol content in the PSVPh copolymer, the lower is the association constant. This trend has also been detected in other PSVPh containing blends in solid state, but at percentage of —OH groups in the copolymer close to 20%. Although the decrease of hydrogen-bond fraction with increasing temperature is a well-established concept,[7] high OH content in PSVPh copolymer blends also leads to weaken in hydrogen bonding due to the reduction of segmental mobilities, which requires not only a suitable distance between complementary functional groups but also specific relative orientations. Nevertheless, in these last two systems, there have been significant interpenetration between unlike polymers, where the space effect described above is predominant over the OH group concentration, as can be concluded from the K_A values calculated for each copolymer sample. Recently, it has been reported that an average value for the dimensionless interassociation equilibrium constant was $K_A = 41$ at 25°C, obtained from extrapolation of FTIR row data employing the association model of Painter and Coleman[7] for a similar PHB–PSVPh polymer blend in solid state.[50] Moreover, it has also been reported by the same research group, using the above procedure,[29] that the values of the equilibrium constant for atactic and for tactic PHB with PVPh homopolymer blends were $K_A = 62.1$ and 38.4, respectively. This disagreement between the K_A values obtained here in solution and those previously reported in solid state for the same polymer blend seems to be a general trend consisting on the K_A values in solution are in most cases greater than those corresponding in solid state. However, despite the differences between the experimental techniques to obtain row data as well as the association models used in both cases, the K_A values estimated here are close to those reported for other polymer blends involving –OH. . . O=C< specific interactions, such as PVPh/poly(vinyl acetate) and PVPh/poly(ε-caprolactone) systems.[7] These results confirm that fluorescence spectroscopy is a powerful tool for accurately measuring
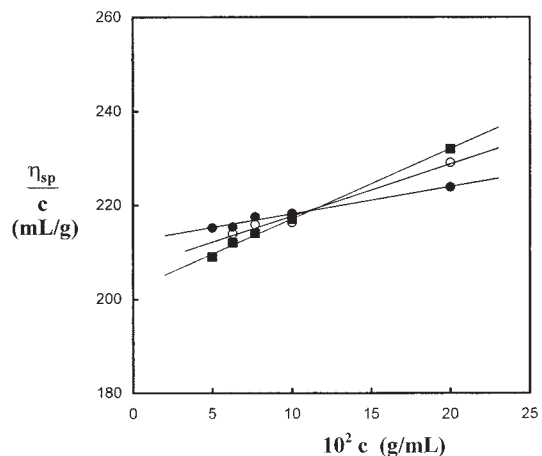

Figure 6 Plots of the reduced viscosity (η_{sp}/c) versus concentration (c) for PHB: (●), pure ECH; (○), ECH + PSVPh(6) at 0.5×10^{-3} g/mL; (■), ECH + PSVPh(6) at 1.0×10^{-3} g/mL (at 25°C).

association constants for polymer mixtures in dilute solution with hydrogen-bonding-specific interactions.

Evidence of complexation from viscometry

Dilute solution viscosity has been considered as one effective technique to investigate polymer–polymer interactions and numerous expressions have been put forward for the prediction of interaction between both polymers. In the present work, we have attempted to apply the method of polymer solvent for the study of compatibility of PHB/PSVPh blend systems.[14,34,37] According to this method, the intrinsic viscosity of a probe polymer, the PHB in our case, in a solution containing a constant concentration of another matrix polymer, such as ECH–PSVPh mixture, can be determined conveniently. Figure 6 shows the plots of reduced viscosity (η_{sp}/c) versus concentration (c) for PHB in pure solvent of ECH and in polymer solvent of [ECH + PSVPh(6)] at 25°C. All the plots are linear in the whole range of concentration used. Moreover, a crossover concentration at $c_3 = 0.10$ g/mL is found. Taking as reference the reduced viscosity values of PHB/ECH binary system, a slight coil shrinkage at [PHB] concentrations lower than c_3 and a coil expansion at concentrations greater than c_3 values can be observed, denoting incompatibility and compatibility, respectively. Extrapolating to zero concentration, the intrinsic viscosity of PHB, $[\eta]_{3,c2}$, can be obtained, being of 212.8 mL/g in pure ECH ($c_2 = 0$), 206.6 mL/g at $c_2 = 0.5 \times 10^{-3}$ g/mL, and 204.4 mL/g at $c_2 = 1.0 \times 10^{-3}$ g/mL, respectively. In light of these results, the intrinsic viscosity of PHB in ECH + PSVPh(6) is less than in pure ECH because a repulsive interaction exist between PHB and PSVPh(6) coils in the polymer solvent. This repulsive interaction increased the intermolecular excluded volume effect, yielding the PHB
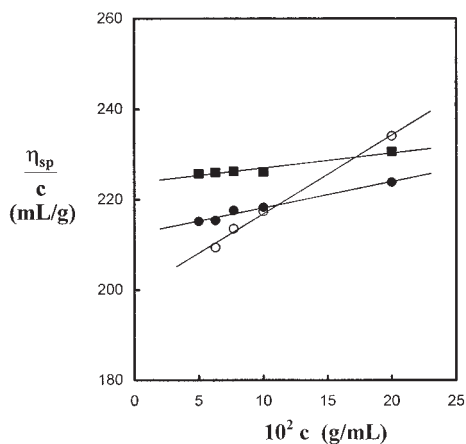
Figure 7 Plots of the reduced viscosity (η_{sp}/c) versus concentration (c) for PHB: (●), pure ECH; (○), ECH + PSVPh(7) at 0.5×10^{-3} g/mL; (■), ECH + PSVPh(7) at 1.0×10^{-3} g/mL (at 25°C).

coil shrinkage in solution and thus the decrease of the intrinsic viscosity of PHB in polymer solvent. Figure 7 shows the plots of reduced viscosity (η_{sp}/c) versus concentration (c) for PHB in pure solvent of ECH and in polymer solvent of [ECH + PSVPh(7)] at 25°C. In this plot, the value of the crossover concentration is similar to that detected in the previous figure; however, for the polymer solvent composition, $c_2 = 1.0 \times 10^{-3}$ g/mL, the reduced viscosity values in the whole PHB concentration range are higher than those of the reference system, meaning coil interpenetration or compatibility. It can also be noticed that the intrinsic viscosity of PHB in [ECH + PSVPh(7)] at $c_2 = 0.5 \times 10^{-3}$ g/mL is 199.4 mL/g, lower than in ECH, as in the preceding TPS. However, the intrinsic viscosity of PHB in [ECH + PSVPh(7)] at $c_2 = 1.0 \times 10^{-3}$ g/mL is 223.7 mL/g, greater than in pure ECH. The more plausible meaning of this behavior is that the attractive hydrogen-bonding-specific interactions between PHB and PSVPh(7) exists in polymer solvent systems at this concentration. These attractive interactions decreased the intermolecular excluded volume effect and consequently the PHB coils can overlap.

The influence of the solvent upon the polymer–polymer interactions also comes from the interaction parameter term Δb, developed from modified Krigbaum and Wall theory.[41] In the framework of this theory, the following equation for mixed polymer solutions is obtained:

$$\eta_{sp,m} = [\eta]_2 c_2 + [\eta]_3 c_3 + b_{22} c_2^2 + 2 b_{23} c_2 c_3 + b_{33} c_3^2 \quad (12)$$

b_{23} represents the mutual intermolecular interactions between the component 2, the PSVPh copolymer, and the component 3, the PHB. According to the nomenclature used throughout the paper, the subindex 1 is assigned to ECH, considered as common solvent. The b_{22} and b_{33} parameters can be obtained from the binary

polymer–solvent subsystems. It is well known that quantitative evaluation of polymer–polymer compatibility from viscosity measurements of TPS has been done from different parameters, such as intrinsic viscosity, Huggins constant, critical concentration, self-association constant, and viscosity slope coefficient or interaction coefficient b. In this study, we consider the b_{23} as a complex interaction parameter in which hydrodynamic, thermodynamic and H-bond associations are included. We try here to explore the PSVPh–PHB compatibility by means of the polymer solvent method, as has been shown in Figures 6 and 7. If specific intermolecular interactions between polymer 2 and 3 take place, a parameter Δb_{23} can be defined as the deviation between both experimental b_{23} and the same parameter theoretically obtained as a combination of the polymer–solvent, b_{22} and b_{33}, viscometric interaction parameters. For the convenience of computation, the specific interaction coefficient for mixed polymer solutions is defined as

$$b_{23} = (b_{22} \times b_{33})^{1/2} \quad (13)$$

However, in some cases the value of either b_{22} or b_{33} can be negative and then the value of b_{23} according to eq. (13) is imaginary. Thus, the Krigbaum and Wall definition of b_{23} becomes unrealistic.[41] For the present context, we have used, instead of eq. (13), a modified form introduced by Castift et al.[51]

$$b_{23}^* = (b_{22} + b_{23})/2 \quad (14)$$

The compatibility of polymer mixture is predicted by a parameter

$$\Delta b_{23} = b_{23} - b_{23}^* = b_{23} - \frac{b_{22} + b_{33}}{2} \quad (15)$$

Notice that b_{23} can experimentally be determined by using eq. (12). Recalling that Δb_{23} was suggested as a criterion to predict polymer–polymer compatibility, $\Delta b > 0$ signifies compatibility, whereas $\Delta b < 0$ indicates incompatibility.[37,52] The numerical Δb_{23} values are compiled in Tables III and IV, for TPS containing PSVPh(7) and PSVPh(6), as a function of both polymer solvent composition, c_2, and R_i, respectively. In both systems positive Δb_{23} values in all the composition range are obtained, showing that the OH content in PSVPh and the consequent hydrogen-bonding density are dominant factors governing the complexation between PHB and PSVPh. In the range of polymer concentrations assayed (10^{-3}–10^{-4} g/mL), ECH exhibit good solvating power for the complex aggregates, forming an stable dispersion. In general, this behavior is in good agreement with those obtained from fluorospectroscopy, although at light of this experimental technique the OH content rather than the space effect

TABLE III
Concentration Dependence of the Mutual Intermolecular Interaction Parameters for ECH/PSVPh(7)/PHB Ternary Polymer System

c_3 (10^2 g/mL)	$c_2 = 1 \times 10^{-3}$ (g/mL)			$c_2 = 0.5 \times 10^{-3}$ (g/mL)		
	R_i (mol/mol)	b_{23} (10^{-2} mL/g)^2	Δb_{23} (mL/g)^2	R_i (mol/mol)	b_{23} (10^{-2} mL/g)^2	Δb_{23} (mL/g)^2
0.0	0.00	85.8	96.0	0.00	80.1	90.3
5.0	0.08	82.3	92.6	—	—	—
6.3	0.11	80.1	90.3	0.22	75.7	85.9
7.7	0.14	77.2	87.4	0.27	79.9	90.1
10	0.18	70.3	80.6	0.35	106.1	116.3
20	0.35	65.3	75.5	0.70	220.0	230.2

seems to be the prevalent factor. Figure 8 (upper part) illustrates the earlier stated, on the contrary, incompatibility between unlike polymers is detected for TPS containing PSVPh (4) copolymer (lower part), where negative values of Δb_{23} were found. Not feasible viscosity data have been obtained for the remaining TPS containing PSVPh (3) or PSVPh (2) copolymer, respectively.

CONCLUSIONS

The five copolymer samples of PSVPh used are completely miscibles with PHB over the composition range reported in epichlorohydrin. It has been proved that, when in a multicomponent polymer system at least one macromolecular component, as the case of PSVPh copolymer, exhibit intrinsic fluorescence, it is not necessary to dope the system with selected probes. Therefore, in this particular case, using a currently available technique such as fluorescence, it is possible to obtain relevant information on the H-bond-specific interactions for PSVPh–PHB–ECH ternary polymer system. Moreover, a simple equilibrium binding model enables us to evaluate an intermolecular equilibrium constant, K_A, coming from steady-state fluorescence data, even though the level of theory utilized in this study is modest compared with available methodology. However, the correlations found demonstrate that even approximate calculations provide affordable and reliable characterizations of interpolymer H-bonding interactions in solution.

At light of the fluorescence results in combination with the association model (see eq. (11)), the following can be concluded: Below 6% vinyl phenol content in the PSVPh copolymer, there is very little amount of inter-(macro) molecular H-bonding, suggesting that the OH groups are unable to find suitable oriented or positioned $>C{=}O$ groups with which to form an intermolecular H-bond. In this case, the absence of specific interactions is confirmed by fluorescence and viscosity measurements. With the first technique, no correlation is found at light of the binding model, and with the second one negative Δb values, as can be seen in Figure 8, confirm the polymer–polymer incompatibility. Above 6% vinyl phenol in the copolymers, both fluorescence and viscometry results show good agreement, revealing that H-bonding-specific interactions take place, enhancing miscibility and compatibility between the PHB and PSVPh copolymer in ECH as common solvent at room temperature. An average interassociation equilibrium constant of $K_A = 8.7$ was found with the binding model described here. This value agrees well with other ones reported for similar polymer pairs compatibilized through hydroxyl–carbonyl hydrogen bonding interactions. The polymer solvent viscometry method has also been used here to obtain complementary evidence of polymer–polymer interactions by means of the Δb_{23} parameter. The vis-

TABLE IV
Concentration Dependence of the Mutual Intermolecular Interaction Parameters for ECH/PSVPh(6)/PHB Ternary Polymer System

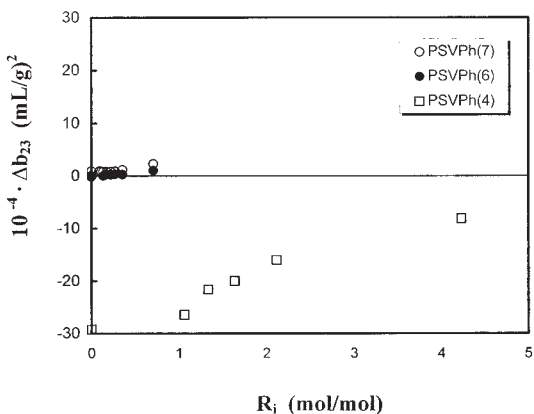| c_3 (10^2 g/mL)	$c_2 = 1 \times 10^{-3}$ (g/mL)			$c_2 = 0.5 \times 10^{-3}$ (g/mL)		
	R_i (mol/mol)	b_{23} (10^{-2} mL/g)^2	Δb_{23} (mL/g)^2	R_i (mol/mol)	b_{23} (10^{-2} mL/g)^2	Δb_{23} (mL/g)^2
0.0	0.00	−5.6	7.4	0.00	−29.1	90.3
5.0	—	—	—	—	—	—
6.3	—	—	—	0.22	10.1	23.3
7.7	0.14	−12.4	0.6	0.27	22.0	35.0
10	0.18	15.1	28.1	0.35	14.0	27.1
20	0.35	17.1	30.2	0.70	87.6	100.6

Figure 8　Plot of the viscometric interaction parameter, Δb_{23}, as a function of the mixed polymer molar ratio, R_i, for different PSVPh samples.

cosity results for these systems, Figure 8 (upper part) where $\Delta b_{23} > 0$, reveal polymer–polymer attractive interactions, confirming that the OH content in PSVPh and the consequent hydrogen bonding density are dominant factors governing the complexation between PSVPh and PHB. This conclusion is in good agreement with that obtained from fluorescence measurements.

References

1. Soria, V.; Figueruelo, J. E.; Abad, C.; Campos, A. Macromol Theory Simul 2004, 13, 441.
2. Gomez, C. M.; Verdejo, E.; Figueruelo, J. E.; Campos, A.; Soria, V. Polymer 1995, 36, 1487.
3. Campos, A.; Gomez, C. M.; García, R.; Figueruelo, J. E.; Soria, V. Polymer 1996, 37, 3361.
4. Panayiotou, C.; Sanchez, I. C. J Phys Chem 1991, 95, 10090.
5. Pimentel, G. C.; McClellan, A. L. The Hydrogen Bond; Freeman: San Francisco, 1960.
6. Cowie, J. M. G.; Arrighi, V. In Polymer Blends and Alloys; Shonaike, G. O.; Simon, G. P.; Eds.; Marcel Dekker: New York, 1999; Chapter 4.
7. Coleman, M. M.; Graf, J. F.; Painter, P. C. Specific Interactions and the Miscibility of Polymer Blends; Technomic Publishing: Lancaster, PA, 1990.
8. Coleman, M. M.; Painter, P. C. Prog Polym Sci 1995, 20, 1.
9. Inoue, T.; Ougizawa, J. Mcromol Sci A Chem 1989, 26, 147.
10. Coleman, M. M.; Painter, P. C. Appl Spectrosc Rev 1984, 23, 255.
11. Hourston, D. J.; Zhang, X. J.; Song, M.; Pollock, M.; Hammiche, A. Thermochim Acta 1997, 294, 23.
12. Mandal, B. M.; Bhattacharyya, C.; Bhattacharyya, N. S. J. Macromol Sci A Chem 1989, 26, 175.
13. Muniz, E. C.; Vazquez, P. A. M.; Bruns, R. E.; Nunes, S. P.; Wolf, B. A. Macromol Chem Rapid Commun 1992, 13, 45.
14. Soria, V.; Figueruelo, J. E.; Campos, A. Eur Polym J 1981, 17, 137.
15. Chee, K. K. Eur Polym J 1990, 26, 423.
16. Timmins, M. R.; Gilmore, D. F.; Fuller, R. C.; Lenz, R. W. Biodegradable Polymers and Packaging; Technomic Publishing: Lancaster, PA, 1993; Chapter 8.
17. Greco, P.; Martuscelli, E. Polymer 1989, 30, 1475.
18. Siciliano, A.; Seves, A.; de Marco, T.; Cimmino, S.; Martuscelli, E.; Silvestre, C. Macromolecules 1995, 28, 8065.
19. Finelli, L.; Sarti, B.; Scandola, M. J Mater Sci A Pure Appl Chem 1997, 34, 13.
20. Gonzalez, A.; Iriarte, M.; Iriondo, P. J.; Iruin, J. J. Polymer 2003, 44, 7701.
21. Avella, M.; Martuscelli, E.; Greco, P. Polymer 1991, 32, 1647.
22. Ikejima, T.; Cao, A. M.; Yoshie, N.; Inoue, I. Polym Degrad Stab 1998, 62, 263.
23. Shuai, X.; He, Y.; Na, Y. H.; Inoue, Y. J Appl Polym Sci 2001, 80, 2600.
24. Ikejima, T.; Yagi, K.; Inoue, Y. Macromol Chem Phys 1999, 200, 413.
25. Ha, C.-S.; Cho, W.-J. Prog Polym Sci 2002, 27, 759.
26. Gestoso, P.; Brisson, J. Comput Theor Polym Sci 2001, 11, 263.
27. Xing, P.; Dong, L.; An, Y.; Feng, Z.; Avella, M.; Martuscelli, E. Macromolecules 1997, 30, 2726.
28. Iriondo, P.; Iruin, J. J.; Fernandez-Berridi, M. J. Polymer 1995, 36, 3235.
29. Iriondo, P.; Iruin, J. J.; Fernandez-Berridi, M. J. Macromolecules 1996, 29, 5605.
30. Porcar, I.; Gomez, C. M.; Perez-Payá, E.; Soria, V.; Campos, A. Polymer 1994, 35, 4627.
31. Vogel, H. FEBS Lett 1981, 134, 37.
32. Thiaudière, T.; Siffert, O.; Talbot, J. C.; Bolard, J.; Alouf, J. E.; Dufourcq, J. Eur J Biochem 1991, 195, 203.
33. Porcar, I.; García, R.; Soria, V.; Campos, A. Polymer 1997, 38, 3545.
34. Soria, V. Gomez, C. M.; Rodríguez, P.; Parets, M. J.; Campos, A. Colloid Polym Sci 1994, 272, 497.
35. Golembiewski, E.; Forty, A.; Curti, E. Polymer 1999, 40, 5129.
36. Quian, J. W.; Miao, Y. M.; Zhang, L.; Chen, H. L. J Membrane Sci 2002, 203, 167.
37. Zhang, Y.; Quian, J.; Ke, Z.; Zhu, X.; Bi, H.; Nie, K. Eur Polym J 2002, 38, 333.
38. Chee, M. J. K.; Ismail, J. Kummerlöwe, C.; Kammer, H. W. Polymer 2002, 43, 1235.
39. Xiang, M.; Jiang, M.; Zhang, Y.; Wu, C. Macromolecules 1997, 30, 5339.
40. Dondos, A.; Benoit, H. Makromol Chem 1975, 176, 3441.
41. Krigbaum, W. R.; Wall, F. T. J Polym Sci 1950, 5, 505.
42. Katri, C. A.; Vaidya, M. M.; Levon, K.; Jha, S. K.; Green, M. M. Macromolecules 1995, 28, 4719.
43. Viswanathan, S.; Dadmun, M. D. Macromolecules 2002, 35, 5049.
44. Gonzalez, A.; Iriarte, M.; Iriondo, P. J.; Iruin, J. J. Polymer 2004, 45, 4139.
45. Gomez, C. M.; Codoñer, A.; Campos, A.; Abad, C. J Colloid Interface Sci 2002, 251, 172.
46. Brinkley, R. L.; Gupta, R. B. AIChE J 2001, 47, 948.
47. Painter, P. C.; Weytsman, B.; Kumar, S.; Shenoy, S.; Graf, J. F.; Xu, Y.; Coleman, M. M. Macromolecules 1997, 30, 932.
48. Gupta, R. B.; Brinkley, R. L. AIChE J 1998, 44, 207.
49. Muthukumaran, P.; Gupta, R. B.; Brinkley, R. L. AIChE J 2002, 48, 386.
50. Gonzalez, A.; Irusta, L.; Fernandez-Berridi, M. J.; Iriarte, M.; Iruin, J. J. Polymer 2004, 45, 1477.
51. Castift, E. H.; Hewtt, W. A. J Appl Polym Sci 1962, 6, 530.
52. Bohmer, B.; Berek, D.; Florian, S. Eur Polym J 1970, 6, 471.